

term in Eq. (3).

For very weak magnetic fields (i.e., the product of the ion cyclotron frequency and the ion collision time is much less than unity, corresponding to the cases considered by the authors in Refs. 1-3), it is stabilizing. However, as the effect of the magnetic field begins to be felt by the ions, we achieve the state where  $\delta_e \mu_i > \delta_i \mu_e$  and the differential drift is destabilizing. In such cases, the ratio of the third to the second terms in Eq. (3) is

$$\frac{(\mu_e - \mu_i)(\delta_e \mu_i - \delta_i \mu_e)}{(\eta_e - \eta_i)(\mu_i \beta_e + \mu_e \beta_i)} \approx \frac{T_e}{T_i}, \quad (4)$$

and therefore this differential-drift destabilizing effect is dominant in plasmas in which  $T_e \gg T_i$ , i.e., in most differentially pumped discharges.

The mechanism of the instability can be understood physically by considering the model shown in Fig. 1. A radially inhomogeneous plasma column of density  $n_0$  develops some helical or kink perturbation as shown in Fig. 1(a). The density is then nonuniform along the magnetic field lines, being higher at point  $P$  than at point  $Q$ . The electrons diffuse easily along the field lines, tending to set up a new equilibrium with point  $P$  positive and point  $Q$  negative. Further development of the instability

is shown at the cross section through  $P$ , in Figs. 1(b) and 1(c). A potential difference now exists across the plasma, producing the electric field  $E$ . For the magnetic field  $B$  as shown, Hall mobilities  $\mu_{eH}$  and  $\mu_{iH}$  drive electrons and ions downward; but  $\mu_{eH} > \mu_{iH}$  for a finite-resistivity plasma column, and a second space-charge separation develops as in Fig. 1(c). The resulting second electric field component  $E_2$  causes a second Hall flow in the  $\vec{E}_2 \times \vec{B}$  direction—in the direction of the original perturbation. We see that this instability will be easy to excite, being driven (in part) and not stabilized by axial electron diffusion. The effect disappears in the limit of no electron-ion-neutral collisions. Then the Hall drift velocity of the electrons and ions becomes equal, and the validity of our partially ionized plasma model breaks down also.

\*This work was supported by the National Science Foundation under Grant No. GK-1165.

†Now at Mt. Auburn Research Associates, Cambridge, Massachusetts.

<sup>1</sup>B. B. Kadomtsev and A. V. Nedospasov, *J. Nucl. Energy*, Pt. C, **1**, 230 (1960).

<sup>2</sup>F. C. Hoh, *Phys. Fluids* **6**, 1184 (1963).

<sup>3</sup>A. Simon, *Phys. Fluids* **6**, 382 (1963).

<sup>4</sup>A. A. Galeev, V. N. Oraevskii, and R. Z. Sagdeev, *Zh. Eksperim. i Teor. Fiz.* **44**, 903 (1963) [translation: *Soviet Phys.-JETP* **17**, 615 (1963)].

## OPTICAL BIREFRINGENCE AND CRYSTAL GROWTH OF HEXAGONAL-CLOSE-PACKED He<sup>4</sup> FROM SUPERFLUID HELIUM\*

O. W. Heybey and D. M. Lee†

Laboratory of Atomic and Solid State Physics, Cornell University, Ithaca, New York

(Received 20 June 1967)

The hexagonal-close-packed (hcp) phase of solid He<sup>4</sup> has exhibited anisotropy in sound-velocity measurements<sup>1,2</sup> and thermal-conductivity measurements.<sup>3</sup> Interpretation of these data requires a knowledge of crystal orientation. Optical birefringence can be used to determine the symmetry axis of hexagonal crystals since the optic axis coincides with the symmetry axis ( $c$  axis). We have made measurements of the difference in the indices of refraction of extraordinary and ordinary light in solid hcp He<sup>4</sup> at temperatures between 1.2 and 1.4°K and pressures between 25.0 and 26.0 atm. We obtain a value  $|n_e - n_o| = (2.6 \pm 0.1) \times 10^{-6}$ . A quarter-wave plate for hcp He<sup>4</sup> at a wavelength of

6328 Å is thus about 6 cm thick.

The sample cells are cylindrical Pyrex glass chambers with flat end windows. Two different cells are used in the experiment, one 5.8 cm in length and the second 2.5 cm long. The solid is formed by slowly increasing the pressure on the liquid helium in the cell, which is completely immersed in the outer helium bath at about 1.2°K, until the freezing pressure is reached. Pressure is applied through vacuum-jacketed capillary tubing provided with appropriate heaters to keep the capillary tubing from blocking with solid. Large crystals (on the order of 2 cm<sup>3</sup>) can be grown in less than 5 min using this technique. Below we present evidence

that many of these are single crystals.

The phase shift  $\delta$  between the fast and the slow axes of the solid helium is related to the difference in the indices of refraction for the extraordinary and ordinary light as shown in Eq. (1):

$$\delta = (2\pi d/\lambda)(n_e - n_o), \quad (1)$$

where  $\delta$  = phase shift between fast and slow axes,  $d$  = length of crystal,  $\lambda$  = wavelength of light used,  $n_e$  = index of refraction for extraordinary light, and  $n_o$  = index of refraction for ordinary light.

We measure  $\delta$  by sending well-collimated linearly polarized light of wavelength 6328 Å from a helium-neon laser into the sample axially along the cell. The direction of the initial polarization can be varied. After passing through the sample, the outgoing light is elliptically polarized and is examined with a quarter-wave plate and a Nicol prism as analyzer to search for a null. The elliptically polarized light is characterized by the direction of the major axis of the ellipse relative to the direction of the initial linear polarization (measured by the angle  $\epsilon$  through which the quarter-wave plate rotates), as well as the ratio of the minor to major axes (measured by the tangent of the difference  $\omega$  in rotation angles of the quarter-wave plate and analyzer). We compensate for the phase shift in the glass by measuring the rotations of the quarter-wave plate and analyzer away from the previously determined positions with no solid helium present in the chamber. This is a good approximation provided that the phase shift produced by the glass is small compared with that produced by the helium as is the case for the maximum value of phase shift which is used to determine  $|n_e - n_o|$ .

Solid helium was formed in the 5.8-cm chamber a total of 36 times with the results shown in Fig. 1. The histogram can be divided into three parts. For 17 cases the rotations of the quarter-wave plate and analyzer are too small to measure reliably, implying that  $\delta$  for these cases is less than 5°. A small value of  $\delta$  can arise from many small crystallites or because the  $c$  axis and therefore the optic axis of a single crystal is along the axis of the chamber. These possibilities cannot be distinguished. Five of the cases show an intermediate phase shift. For 14 cases the phase shift is larger than 70°, with the largest observed value being 85°.

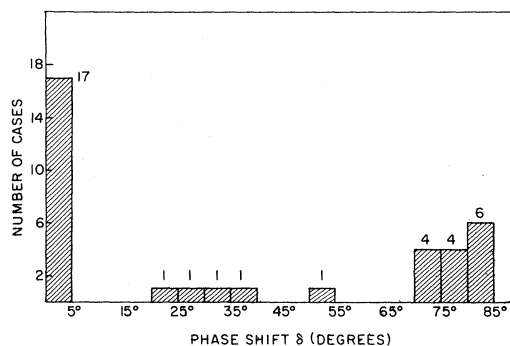


FIG. 1. A histogram of data taken with a 5.8-cm-long optical chamber showing the number of solid samples corresponding to successive phase shift intervals of 5°. The maximum  $\delta$  is 85° for the 5.8-cm chamber.

We take  $\delta = 85^\circ$  as a real maximum (implying that for this case the  $c$  axis of the crystal is perpendicular to the light beam), and calculate  $n_e - n_o$  from Eq. (1), getting  $|n_e - n_o| = (2.6 \pm 0.1) \times 10^{-6}$ . The uncertainty arises from an estimated  $\pm 2^\circ$  uncertainty in the 85° and a  $\pm 0.1$ -cm uncertainty in the length of the chamber. The maximum observed phase shift scales linearly with cell size as shown by measurements with the 2.5-cm chamber. If 85° is the true maximum for the large chamber, a scaling law would predict that the maximum phase shift should be 37° in the 2.5-cm cell, in good agreement with the observed value of 35°.

We have a number of indications that the solid sample is frequently a single crystal. The scaling law described above is evidence that, at least for the larger phase shifts, the light beam traverses only one crystal. Secondly, the outgoing elliptically polarized light shows, in most cases, the relationship between  $\epsilon$  and  $\omega$  as a function of initial polarization direction expected for a single crystal. Finally, six different crystals consecutively grown in the 2.5-cm cell on a particular day showed identical rotations of quarter-wave plate and analyzer, an unlikely situation if several crystals were present simultaneously. These results suggest that a single crystal with the same preferred orientation was formed during each of the six solidifications possibly because of the presence of some contamination in the chamber forming a nucleation center. On thermal recycling, an entirely different phase shift and hence an entirely new orientation was obtained.

We conclude that the difference in the indices of refraction for extraordinary and ordinary light for helium crystals (grown at pressures

below 26 atm is  $|n_e - n_o| = (2.6 \pm 0.1) \times 10^{-6}$ . Rather large single crystals of solid helium can be grown quickly by increasing the pressure over superfluid helium to slightly above the freezing pressure.

Note added in proof.—We have recently received preprints of papers by J. E. Vos, R. Veenenga Kingma, F. J. van der Gaag, and B. S. Blaisse of Delft, The Netherlands, which have been accepted for publication by Phys. Letters and Physica. They performed similar measurements on small (2-mm linear dimension) solid-helium crystals using a somewhat different technique and their results at 30 atm are in good agreement with the present results. Using crossed beams they were able to show that  $n_e - n_o$  is positive for hcp solid helium and to measure the direction of the  $c$  axis for sever-

al arbitrary crystals.

We wish to acknowledge many helpful discussions with Professor G. V. Chester, Professor P. L. Hartman, Professor H. Mahr, and Dr. F. P. Lipschultz. We are grateful to Dr. Bernard Bertman for useful suggestions during the preparation of the manuscript.

\*Work supported by the National Science Foundation and the Advanced Research Projects Agency through the Materials Science Center of Cornell University.

†John Simon Guggenheim Memorial Fellow on leave at Brookhaven National Laboratory during the academic year 1966-1967.

<sup>1</sup>F. P. Lipschultz and D. M. Lee, Phys. Rev. Letters **14**, 1017 (1965).

<sup>2</sup>J. H. Vignos and H. A. Fairbank, Phys. Rev. **147**, 185 (1966).

<sup>3</sup>B. Bertman, H. A. Fairbank, C. W. White, and M. J. Crooks, Phys. Rev. **142**, 74 (1966).

## EXACT SOLUTION OF THE TWO-DIMENSIONAL SLATER KDP MODEL OF A FERROELECTRIC

Elliott H. Lieb\*

Physics Department, Northeastern University, Boston, Massachusetts

(Received 31 May 1967)

The Slater KDP model is solved for all temperatures and with an electric field. Above  $T_C$  the specific heat behaves like  $(T - T_C)^{-1/2}$  and the polarizability like  $(T - T_C)^{-1}$ . There is a first-order phase transition at  $T_C$  (latent heat). Below  $T_C$  the free energy is simply  $-|\mathcal{E}|d$  ( $\mathcal{E}$  = electric field,  $d$  = dipole moment).

Slater<sup>1</sup> introduced a model of hydrogen-bonded ferroelectrics known as the KDP model, since it was supposed to account for  $\text{KH}_2\text{PO}_4$  and similar substances. He treated the model by mean field theory and obtained a first-order phase transition (latent heat). The position of the critical temperature  $T_C$  and the value of the latent heat were shown to be correct by Takahashi.<sup>2</sup> The model has been widely discussed.<sup>3</sup>

Recently, Wu<sup>4</sup> gave an exact treatment of a modified version of the two-dimensional Slater model. He obtained the same  $T_C$  as Slater but found a second-order phase transition (no latent heat). Wu also found that the specific heat  $C$  was 0 for all  $T < T_C$  and  $C \sim (T - T_C)^{-1/2}$  near and above  $T_C$ . This contrasts with Slater's result that  $C$  is finite at  $T_C$ .

In this paper we give an exact solution of the original Slater model in two dimensions. We also wish to emphasize that the analysis is somewhat different above and below  $T_C$  and that we have solved the model in both temperature ranges. Our results are the following:

(1) Below  $T_C$ ,  $C = 0$  as found by Wu. (2) There is a latent heat at  $T_C$  which agrees with Slater's value. (3)  $C \sim (T - T_C)^{-1/2}$  near and above  $T_C$ , which agrees with Wu. (4) Near and above  $T_C$  the polarizability goes like  $(T - T_C)^{-1}$ , which agrees with Slater's treatment (Wu did not discuss the polarizability of his model).

The mathematical statement of the problem is to place arrows on the bonds of a square  $N \times N$  net so that precisely two arrows point into each vertex. Associated with the six allowed vertices (Fig. 1) are energies  $e_1 = e_2 = 0$ ,  $e_3 = e_4 = e_5 = e_6 = \epsilon > 0$ . In the  $F$  model of an antiferroelectric discussed previously,<sup>5</sup> the assignments were  $e_1 = e_2 = e_3 = e_4 = \epsilon > 0$ ,  $e_5 = e_6 = 0$ .

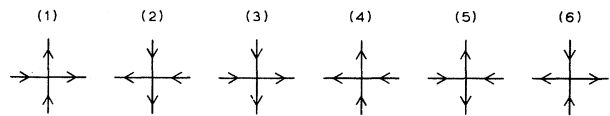


FIG. 1. The six allowed vertex configurations for the Slater KDP model in two dimensions. The energies are  $e_1 = e_2 = 0$ ;  $e_3 = e_4 = e_5 = e_6 = \epsilon > 0$ .